Anal. Chem. **2009,** *81,* 7321–7325

Electro-Coalescence of Digitally Controlled Droplets

Xize Niu,[†,‡] Fabrice Gielen,[‡] Andrew J. deMello,*[,†] and Joshua B. Edel*[,†,‡]

Department of Chemistry, and Institute of Biomedical Engineering, Imperial College London, Exhibition Road, South Kensington, London SW7 2AZ, United Kingdom

In this paper we describe a universal mechanism for merging multiple aqueous microdroplets within a flowing stream consisting of an oil carrier phase. Our approach involves the use of both a pillar array acting as a passive merging element, as well as built-in electrodes acting as an active merging element. The pillar array enables slowing down and trapping of the droplets via the drainage of the oil phase. This brings adjacent droplets into close proximity. At this point, an electric field applied to the electrodes breaks up the thin oil film surrounding the droplets resulting in merging.

Downloaded via ETH ZURICH on April 5, 2019 at 22:39:59 (UTC).
See https://pubs.acs.org/sharingguidelines for options on how to legitimately share published articles.

In the past decade, droplet based microfluidic systems have drawn much attention in the scientific community.[1−8] For example, it has recently been shown that reactions and biological assays within these small nano- to pico- liter sized droplets can be performed and detected on a microsecond time scale.[9] Such applications often require fusion or mixing of droplets to study reactions or assays to completion. With this in mind, reproducible and selective merging of droplets is needed to ensure precise and accurate delivery of a particular analyte or solvent. This is especially true for large scale applications where multiple reagents are involved[10] and for systems where hydrodynamic instabilities in droplet delivery induce irregularities in the merging of droplets.

Different approaches have been demonstrated to successfully merge droplets. These include, the use of electric fields,[11−14] magnetic nanoparticles[15] electrorheological conditions,[16] optical components,[17] or by the use of either patterned surfaces or microfluidic structures.[18−20] All these merging techniques utilize either passive or active merging approaches. Importantly, passive approaches have the ability to adjust the spatial distribution of the droplets by controlling the aqueous and oil regional flow fields. On the other hand, active approaches rely on initiating a sufficiently strong disturbance between neighboring droplets to achieve merging. For example, electrocoalescence can be used where the disturbance is initiated by applying an electric field. Interestingly this mechanism has yet to be fully understood, and there are still debates as to the underlying merging mechanism.[12,13,21] What is clear is that active components are especially useful in applications where surfactants are used to stabilize droplets over long time periods.[22] In the presence of surfactant, droplets tend not to merge even if they are tightly compressed unless an electric field is applied.

In this paper, we combined the advantages of both passive and active merging approaches, to create a novel merging element which can merge droplets regardless of droplet content. It should be noted, that Frenz et al. amongst others have already shown electrical field induced droplet fusion within an expansion channel;[23] however, our approach offers significant advantages which include the ability to adjust the interdroplet distance in a facile manner, precisely control of the number and sequence of droplets being merged, and finally achieve efficient merging under high surfactant concentrations.

* To whom correspondence should be addressed. E-mail: a.demello@imperial.ac.uk (A.J.deM.), joshua.edel@imperial.ac.uk (J.B.E.).
† Department of Chemistry.
‡ Institute of Biomedical Engineering.

(1) Huebner, A.; Sharma, S.; Srisa-Art, M.; Hollfelder, F.; Edel, J. B.; Demello, A. J. *Lab Chip* **2008**, *8*, 1244–1254.
(2) Engl, W.; Roche, M.; Colin, A.; Panizza, P.; Ajdari, A. *Phys. Rev. Lett.* **2005**, *95*, 208304.
(3) Thorsen, T.; Roberts, R. W.; Arnold, F. H.; Quake, S. R. *Phys. Rev. Lett.* **2001**, *86*, 4163–4166.
(4) Song, H.; Chen, D. L.; Ismagilov, R. F. *Angew. Chem., Int. Ed.* **2006**, *45*, 7336–7356.
(5) Anna, S. L.; Bontoux, N.; Stone, H. A. *Appl. Phys. Lett.* **2003**, *82*, 364–366.
(6) Cristobal, G.; Benoit, J. P.; Joanicot, M.; Ajdari, A. *Appl. Phys. Lett.* **2006**, 89.
(7) Dollet, B.; van Hoeve, W.; Raven, J. P.; Marmottant, P.; Versluis, M. *Phys. Rev. Lett.* **2008**, 1.
(8) Hsiung, S. K.; Chen, C. T.; Lee, G. B. *Journal of Micromechanics and Microengineering* **2006**, *16*, 2403–2410.
(9) Song, H.; Ismagilov, R. F. *J. Am. Chem. Soc.* **2003**, *125*, 14613–14619.
(10) Jeffries, G. D. M.; Kuo, J. S.; Chiu, D. T. *Angew. Chem., Int. Ed.* **2007**, *46*, 1326–1328.
(11) Ahn, K.; Agresti, J.; Chong, H.; Marquez, M.; Weitz, D. A. *Appl. Phys. Lett.* **2006**, 88.
(12) Herminghaus, S. *Physical review letters* **1999**, *83*, 2359–2361.
(13) Priest, C.; Herminghaus, S.; Seemann, R. *Appl. Phys. Lett.* **2006**, 89.
(14) Sgro, A. E.; Allen, P. B.; Chiu, D. T. *Anal. Chem.* **2007**, *79*, 4845–4851.
(15) Nguyen, N. T.; Ng, K. M.; Huang, X. Y. *Appl. Phys. Lett.* **2006**, 89.
(16) Niu, X. Z.; Zhang, M. Y.; Wu, J. B.; Wen, W. J.; Sheng, P. *Soft Matter* **2009**, *5*, 576–581.
(17) Baroud, C. N.; de Saint Vincent, M. R.; Delville, J. P. *Lab Chip* **2007**, *7*, 1029–1033.
(18) Tan, Y. C.; Fisher, J. S.; Lee, A. I.; Cristini, V.; Lee, A. P. *Lab Chip* **2004**, *4*, 292–298.
(19) Bremond, N.; Thiam, A. R.; Bibette, J. *Phys. Rev. Lett.* **2008**, 1.
(20) Niu, X. Z.; Gulati, S.; Edel, J. B.; deMello, A. J. *Lab Chip* **2008**, *8*, 1837–1841.
(21) Mostowfi, F.; Khristov, K.; Czarnecki, J.; Masliyah, J.; Bhattacharjee, S. *Appl. Phys. Lett.* **2007**, *90*, 3.
(22) Holtze, C.; Rowat, A. C.; Agresti, J. J.; Hutchison, J. B.; Angile, F. E.; Schmitz, C. H. J.; Koster, S.; Duan, H.; Humphry, K. J.; Scanga, R. A.; Johnson, J. S.; Pisignano, D.; Weitz, D. A. *Lab Chip* **2008**, *8*, 1632–1639.
(23) Frenz, L.; El Harrak, A.; Pauly, M.; Begin-Colin, S.; Griffiths, A. D.; Baret, J. C. *Angew. Chem., Int. Ed.* **2008**, *47*, 6817–6820.

10.1021/ac901188n CCC: $40.75 © 2009 American Chemical Society
Published on Web 07/21/2009

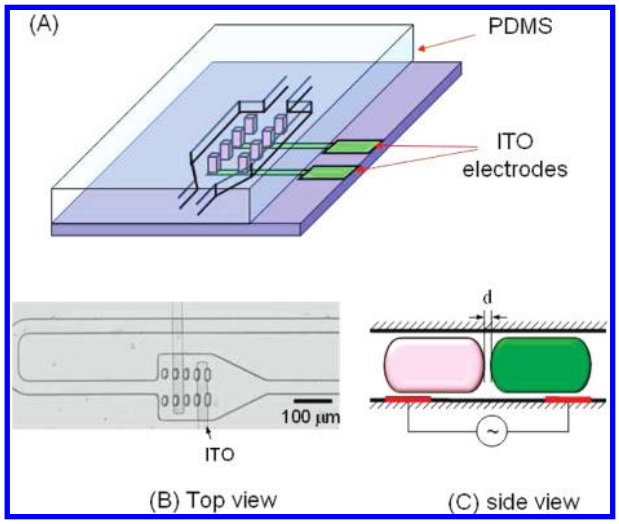

Figure 1. (A) Schematic of the merging chamber. (B) Bright field optical image of the merging chamber. (C) Cross sectional schematic of two droplets being merged.

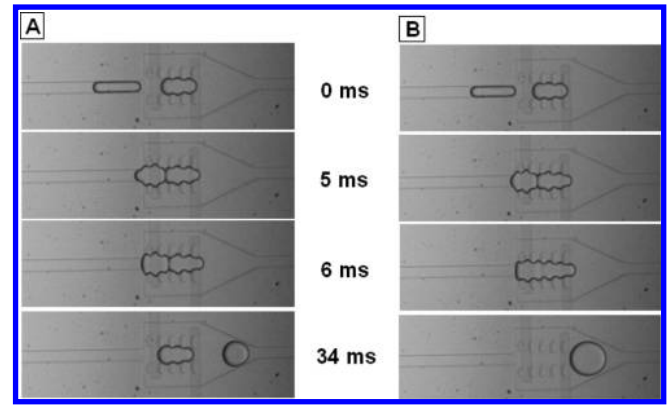

Figure 2. Merging device during operation. (A) In the absence of electric field, the droplets, containing surfactant, entering the merging chamber do not merge. (B) With an applied electric field, the droplets entering the chamber coalesce.

EXPERIMENTAL SECTION

A schematic of the fluidic chip design and operating mechanism is shown in Figure 1. The fluidic channels have a 50 × 50 μm rectangular cross section and dilate to a width of 250 μm. This wider chamber is effectively the heart of the "merging element". This chamber consists of two parallel pillar arrays. The size and location of the pillars were designed to ensure that droplets of similar size can be slowed down and trapped between the two sets of pillars. The pillars have a 20 μm square cross section and a pitch of 36 μm. Also embedded within the merging chamber are two parallel indium tin oxide (ITO) electrodes, which were integrated onto the lower substrate. These electrodes were designed to run perpendicular to the pillars. The distance between electrodes was designed to be either 100 or 200 μm (Figure 1b). By applying an alternating current (AC) electric field to the ITO electrodes, the interface between the trapped droplets within the chamber element is ruptured resulting in complete merging.

The fluidic channel and pillars were fabricated from polydimethylsiloxane (PDMS) using standard soft lithographic techniques. More specifically, to fabricate the microfluidic chip, PDMS base and curing agent (Sylgard 184; Dow Corning, Wiesbaden, Germany) was mixed in a ratio of 10:1 w/w, degassed and decanted onto an SU-8 master. The resulting structure was cured overnight in an oven at 65 °C. After thermal curing, the polymer layer was peeled off the master. This was followed by inlet and outlet holes being punched through the reservoirs. The device was sealed with ITO coated glass. Prior to sealing, the ITO layer (100 nm thick) was patterned using standard lithographic techniques to fabricate the electrodes (Figures 1b and 1c). Importantly, ITO has the added advantage of being optically transparent; therefore droplets could easily be observed directly above the electrodes. The substrates were cleaned and plasma treated, and finally, the two layers were manually aligned and bonded under an optical microscope.

In initial experiments, hexadecane oil (Sigma-Aldrich) was used as the continuous phase with Span 80 added at various concentrations to act as a surfactant. All experiments were performed at room temperature. Deionized water or deionized water containing a small amount of food dye was used as the discrete aqueous phase. Syringe pumps (PHD 2000, Harvard Apparatus) were used to pump fluids into the microfluidic channels at total flow rates ranging from 1−10 μL/min. Droplet generation frequencies up to 300 Hz could be achieved with our current platform. A high speed camera (Phantom, v5.1, Vision Research) was used for data acquisition, and Matlab was used to analyze and process recorded images.

Figure 2 shows an optical image of the microfluidic device during operation. On the left-hand column of Figure 2, no electric field was applied to the electrodes. At time 0 ms, a static droplet is trapped within the pillar array. A flowing droplet generated upstream arrives at the entrance of the merging chamber after 5 ms. As the second droplet gets pushed further into the array, the first droplet is expelled without any merging taking place due to the presence of surfactant. On the other hand, Figure 2b depicts a similar scenario; however, this time with an electric field applied to the electrodes. As in the previous case after 5 ms the second droplet approaches the first trapped droplet within the array and after 6 ms, the two droplets fuse together. This is followed by the newly formed droplet departing the merging chamber after 34 ms. The next part of the manuscript describes the differences between the mechanisms leading to merging and non-merging, respectively.

Merging Mechanism and Calibration. It has previously been shown by Mostowfi et al. that the rupture potential inducing coalescence of droplets is linearly dependent on the separation distance between the droplets.[24] In our design where the pillar array ensures drainage of the oil phase between the droplets, the voltage needed to rupture the interface can be as low as 50 V/mm, instead of 500 V/mm as has been previously reported.[11] To precisely determine the exact conditions in terms of voltage, amplitude, and frequency at which point coalescence occurs, the device was calibrated using different concentrations of surfactant (Span-80), ranging from 0 to 0.5 w/w %. Here hexadecane was used as carrier phase and deionized water as the discrete phase. The size of the droplets created by our T-junction was adjusted by varying the flow rates so that the droplets would be approximately 200 μm in length and 50 μm wide. These dimensions

(24) Ruckenst., E.; Jain, R. K. *Journal of the Chemical Society-Faraday Transactions Ii* **1974**, *70*, 132–147.

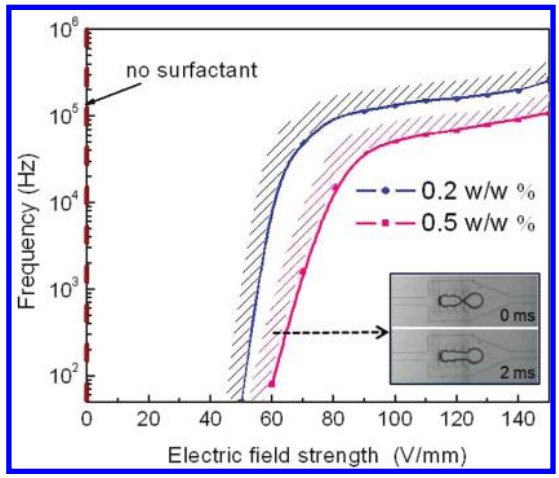

Figure 3. Calibration diagram of the merging threshold as a function of voltage and frequency.

were chosen so that the passive merging chamber could contain anywhere from 2−4 droplets at any given time.

The curves shown in Figure 3 delimitate transition regions between coalescence and non-coalescence of all droplets in the presence of 0, 0.2, and 0.5 w/w% surfactant. The threshold voltage required to cause coalescence scales up with the surfactant concentrations which is consistent with the fact that surfactants generally improve droplet stability. Without any surfactant present, all droplets within the pillar array merge under no applied electric field. A purely passive merger such as this has been studied in depth and published by the authors in 2008.[20] However, when a surfactant concentration of 0.2 and 0.5 w/w% was used, a clear trend in the applied electric field can be seen as a function of operating frequency. Any conditions to the right of these curves will result in droplets being merged. Within the hatched transition areas in Figure 3, merging is either not reproducible or merges via decompression.[19] An image demonstrating this process is shown in the inset within Figure 3. At voltages well above threshold with frequencies lower than 10−100 kHz, electrocoalescence events always occur between the patterned electrodes. Importantly, no failure in merging was observed under continuous operation of the device for several hours. Interestingly, at frequencies above 100−500 kHz, no coalescence was seen.

Thickness of the Oil Interface at Merging. The oil membrane thickness between droplets is not only crucial to further understand droplet merging, but also important for reagent exchange and diffusion between droplets. It is generally a difficult task to optically observe and measure this thickness (typically less than 1 μm) prior to merging. Our merging chamber provides a platform to slow down the droplets sufficiently to study the oil membrane thickness between two microdroplets. More specifically, the oil drainage rate between the droplets can be deduced theoretically and verified with a high speed camera. The average membrane thickness at the time of merging can then calculated from the drainage rate.

A detailed observation of the merging process in Figure 2 shows that the first droplet in the merging chamber will reach a Newtonian force balance, and is trapped and stopped before merging with the succeeding droplet. The succeeding droplet, sustains a hydraulic pressure from the oil pushing it forward (compared with the flow direction) and an inner pressure from

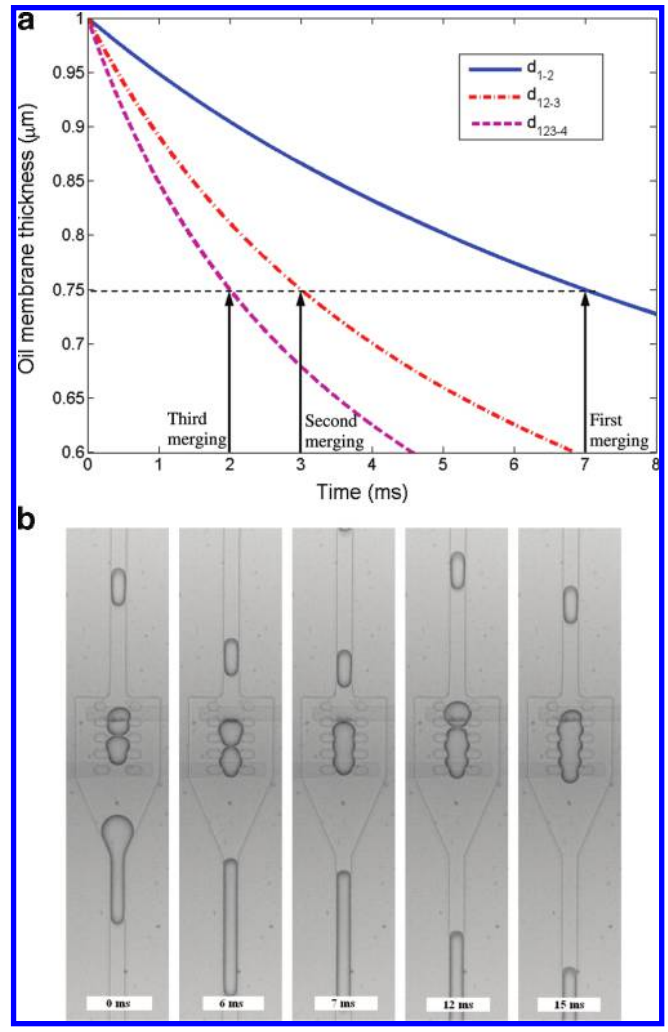

Figure 4. (A) Calculated oil film membrane thickness as a function of time for three successive droplet merging events. d_{1-2} indicates thickness of the oil interface between the first and second droplet. d_{12-3} indicates the thickness of the oil interface between the third droplet entering the chamber and the merged d_{1-2} droplet. Finally, d_{123-4} indicates the thickness of the oil interface between the third droplet entering the chamber and the merged d_{12-3} droplet. The arrows indicate the experimental merging time for the three successive merging events. The intersections between the experimental and theoretical results indicate a film thickness of 750 nm. (B) Time sequence of 3 droplets being merged.

the surface tension pushing it backward. The pressure balance can be described as follows[20]

$$\Delta P = \Delta P_{\mathrm{h}} - \Delta P_{\mathrm{d}} \qquad (1)$$

where ΔP_{h} is the hydraulic pressure and ΔP_{d} the inner pressure. To infer a realistic value for ΔP, we simulated droplet accumulation in the merging chamber using the Comsol simulation package. The results suggest that the pressure at the inlet of the chamber is around 600 Pa. The oil film drainage rate between the two droplets can therefore be derived from the Reynold's equation and can be written as follows:

$$\mathrm{d}(1/D^2)/\mathrm{d}t = a\Delta P, \quad a = 4/(3\eta r^2) \qquad (2)$$

Here D is the interface thickness, t the time, η the dynamic viscosity, and r the radius of the droplet. The merging chamber

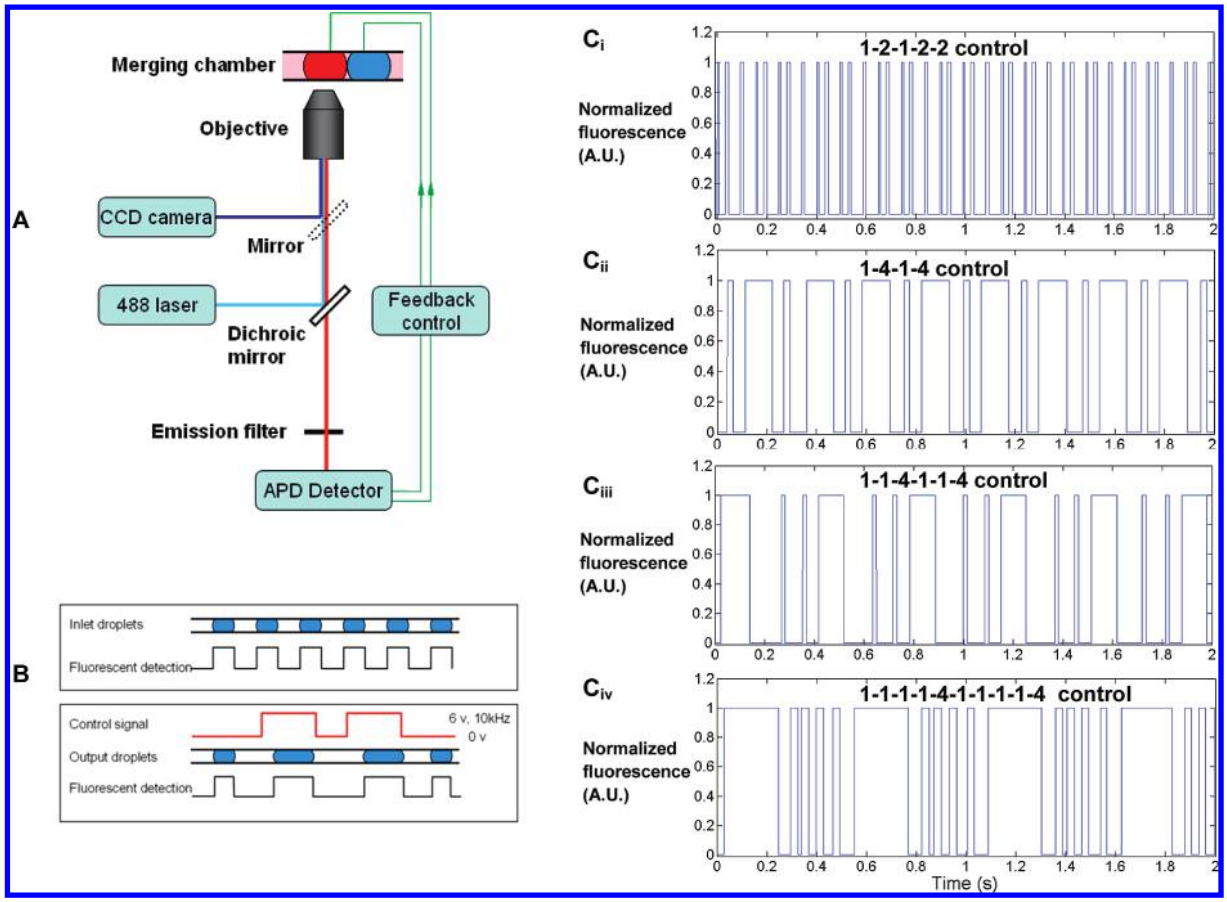

Figure 5. (A) Schematic of the optical setup used for selective merging of droplets. (B) Schematic of the detected fluorescence signal with and without the use of feedback control. (C) Normalized fluorescence signal obtained by merging droplets in the following sequence: (i) 1−2−1−2−2, (ii) 1−4−1−4, (iii) 1−1−4−1−1−4, (iv) 1−1−1−1−4−1−1−1−1−4.

was designed to merge up to four consecutive droplets (via three separate merging events). As a result, differences in the oil drainage rate can be monitored. As the droplet increases in size as does the differential pressure ΔP resulting in a faster oil drainage rate. This can be seen in Figure 4a where a plot is shown correlating the oil membrane thickness as a function of time using eq 2 for three successive merging events. The interface thickness for these three merging events is defined as d_{1-2}, d_{12-3}, and d_{123-4} respectively. Movies with 100 ns frame times were used to verify that no abrupt acceleration or deceleration takes place during the merging process. This effectively confirms that eq 2 remains valid prior to merging taking place.

Moreover, experimental snapshots of the merging events enabled characterizing the merging time based on the number of droplets present in the pillar chamber (Figure 4b). The merging time was defined as the time elapsed between droplets 1 μm apart and their merging. For example, the merging time decreases from 7 ms (between 0 and 7 ms, in Figure 4b) for the first pair of droplets to 3 ms for the second pair (between 12 and 15 ms). Average merging times are denoted by arrows as is shown in Figure 4a. This intercept also highlights the oil film thickness prior to merging. Interestingly, we found that from Figure 4a, that all merging events take place when droplets are approximately 750 nanometers away from each other. Such a distance is much larger than the commonly assumed several nanometers[25] derived from the distance of two monolayers of surfactant molecules.

Selective Merging for Digital Reactions. The electric field applied to the ITO electrodes can be easily computer controlled or programmed by a function generator to selectively merge droplets, in a systematic manner flowing through the merging chamber. Importantly, this can find applications in controlled sequential reactions[4,10] or droplet logic.[26] We experimentally verify the feasibility of this by doping the aqueous droplets with a 1 mM fluorescein solution. The fluorescence signal detected at a single point in the middle of the merging chamber was recorded, and the intensity was used as a feedback mechanism to precisely control the number of droplets being merged. The schematic of the optical setup is shown in Figure 5a. Briefly, a 488 nm laser beam excitation source is focused into the microfluidic channel with a 20× objective. The emitted photons are collected using the same microscope objective, and the fluorescence light is focused onto an avalanche photodiode detector. Figure 5b shows a schematic of the process. Initially a train of uniformly spaced droplets are introduced into the merging chamber (Figure 5b, top). Once in the chamber, the fluorescence signal can be read out, and merging can be subsequently achieved by triggering the function generator to apply an electric field to the ITO electrodes. Patterns such as those shown in the bottom of Figure 5b can be generated to perform alternate merging or merging with a well-defined number of droplets.

(25) Leneveu, D. M.; Rand, R. P.; Parsegian, V. A.; Gingell, D. *Biophys. J.* **1977**, *18*, 209–230.
(26) Cheow, L. F.; Yobas, L.; Kwong, D. L. *Appl. Phys. Lett.* **2007**, 90.

Figure 5c$_i$ shows experimental results of the optical signal when the laser beam was focused at the outlet point of the merging chamber. In this case, the control signal was delivered using a sinusoidal waveform at a frequency of 10 kHz, over a 2 s acquisition time. After merging, the detected width of the fluorescence peak increases by a factor of 2, which implies successful merging (the fluorescence signal was normalized for visualization purposes). In the second example (Figure 5c$_{ii}$−c$_{iv}$), a series of four droplets are merged in varying sequences in a reproducible manner. In both examples, no perturbation in droplet size and spacing was found. Such selective merging can be nicely coupled to a passive sorting approach to collect fused droplets based on droplet size.[18,26] These merging examples demonstrate the capabilities of the platform to selectively merge up to four droplets in a reproducible manner.

CONCLUSION

We have engineered a system capable of selective merging one or more aqueous microdroplets in a reproducible manner. The hybrid platform exploits the advantage of both passive and active merging mechanisms. The chip was designed to permit low voltage coalescence events. Although the merging of droplets, in this paper, was predominantly performed using hexadecane, Span 80, and DI water, other combinations were also tested. For example, FC-40 with 1.8% (w/w) E2K0660 surfactant[22] was used as the oil phase and 20 nM streptaviden labeled with alexa 488 (Invitrogen, Paisley, U.K.) was used as the aqueous phase. Importantly, changing of the droplet and oil conditions did not affect droplet merging. The platform described in this paper will prove to be especially useful in applications where merging a well defined number of droplets in required. Importantly, this platform also offers significant advantages where surfactants are added to the oil phase in order to stabilize the system. Potential applications include sequential chemical/biological reactions and assays (e.g., cascade reactions), manipulation of elastic lipid vesicles, droplet logics, and droplet sorting.

ACKNOWLEDGMENT

This work was supported by the RCUK Basic Technology Programme. We would like to thank Miss Mengying Zhang from HKUST for helpful discussions on oil/water emulsions.

SUPPORTING INFORMATION AVAILABLE

Additional information in the form of AVI files. This material is available free of charge via the Internet at http://pubs.acs.org.

Received for review June 1, 2009. Accepted July 6, 2009.

AC901188N